

STATUS OF A 3.2 T SUPERCONDUCTING WIGGLER AT NSRRC

C. S. Hwang*, C. H. Chang, H. P. Chang, J. R. Chen, H. H. Chen, J. Chen, W. S. Chiou, Y. C. Chien, T. C. Fan, C. C. Kuo, F. Y. Lin, H. C. Li, S. N. Hsu, K. T. Hsu, M. H. Huang, G. Y. Hsiung, F. Z. Hsiao

NSRRC, 101 Hsin-Ann Road, Science-Based Industrial Park, Hsinchu 30077, Taiwan

Abstract

A 3.2 T superconducting wiggler (SW6) with a periodic length of 6 cm and 32 poles was designed and fabricated as an X-ray source. A 1.4056 m long special aluminum beam duct with stainless steel taper and flange was developed and constructed to suit the ultra-high vacuum condition of the electron beam. Two measurement systems – involving a room temperature and a cryogenic Hall probe were designed to measure the field of the SW6. Furthermore, a cryogenic plant that is used to supply liquid helium and nitrogen to the SW6 has already been designed and established.

1. Introduction

The NSRRC storage ring has four 6 m long straight sections in which the insertion devices are installed. Currently, no extra straight section is used for installing any insertion device. However, a superconducting insertion device, a 3.2 T SW6 with a 6 cm period [1,2], has recently be designed and constructed, in response to the growing demand for X-ray research. The SW6 located down stream of the superconducting RF cavity in the fourth straight section and was installed in the storage ring in the middle of January 2004. It was tested successfully at the end of April 2004.

Table 1 : Specifications of the SW6 Magnet.

Number of period	16
Physical length (cm)	140.6
Magnet period (cm)	6.4
Magnet total dimension LxWxH (cm)	135x120x 208
Horizontal (vertical) aperture of beam duct (cm)	8 (1.1)
LHe boiling off (l/h)	2.5
Beam duct temperature (K)	300 - 100
Peak filed (T)	≥ 3.2
Average excitation rate (A/s)	≥ 0.8
Deflection parameter $K=0.934B\lambda$	≥ 19.1
Radiation angle (mrad.) (68% of flux @ 0 mrad & 15 keV)	$\pm 6 (\pm 3)$
Electron beam size and divergence $\sigma_x (\sigma_y), \sigma'_x (\sigma'_y)$ (mm), (mrad)	0.46(0.065), 0.044(0.022)
Photon beam size and divergence $\sigma_{rx} (\sigma_{ry}), \sigma'_{rx} (\sigma'_{ry})$ (μm), (mrad) @ 15 keV	0.01(0.04), 0.86(0.17)
Photon flux (brilliance) @ 15 keV (0.5A)	6.5×10^{13} (1.2×10^{15})
Total power (kW) @ 500 mA	6.4

Table 1 lists the main specifications of the SW6 and Fig. 1 compares the spectral flux of the entire X-ray source in the NSRRC storage ring. The flux of X-rays between 2 and 28 keV from the SW6 that exceeded that from other insertion devices. The on-axis magnetic field was measured at room temperature using a Hall probe. The measurements reveal that the first and second field integrals are quite consistent with the designed values. A cryoplant will be built to provide liquid helium to the superconducting wigglers. Meanwhile, the cryoplant can be switched to provide liquid helium to the superconducting RF (SRF) cavity, to maintain the operation of the SRF cavity and provide backup in the

* e-mail: cshwang@nsrrc.org.tw

case of damage of the SRF cryoplant. Nowadays, the SRF cryogenic system is used to provide liquid helium and nitrogen to the SW6 for testing and commissioning the magnet. The SRF cryogenic system with a maximum liquefaction rate of 139 L/h provides liquid helium to the SW6 magnet at an operating pressure of 1.25 bars. Magnet testing and commissioning results show that there are thirteen quenches to obtain the nominal field of 3.2 T at the excitation of 285 A. The electron beam pass through SW6 and keep at stable orbit without any trim coil compensation. This work describes the mechanical design of the SW6, the aluminum beam duct, the magnetic field measurement, the cryogenic plant and the results of commissioning the magnet at the cryogenic plant.

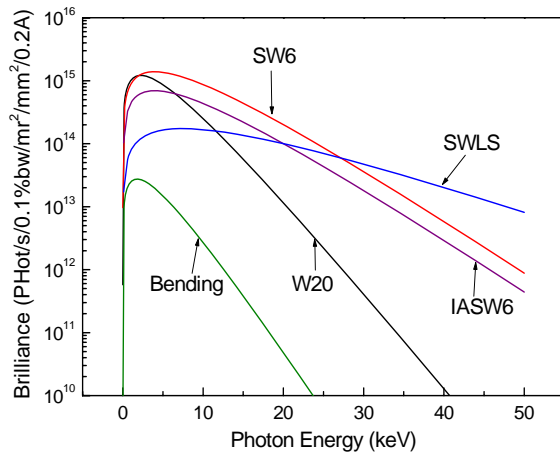


Fig.1. Photon brilliance spectra of NSRRC ID X-Ray source.

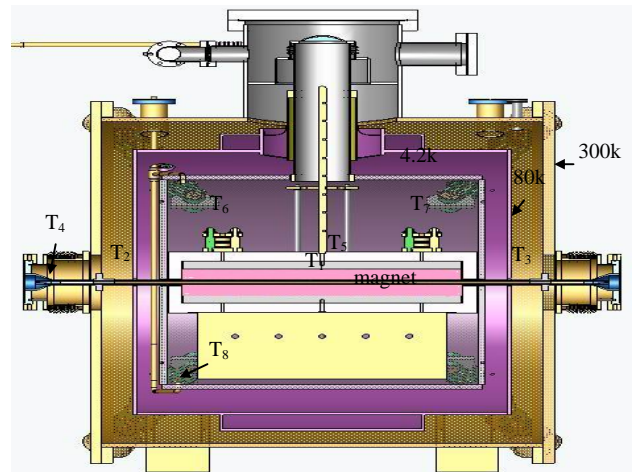


Fig.2. 3-D design and mechanical components of SW6.

2. Construction and performance of magnet

The construction of the magnet involves coils, iron poles, return yokes, quench protection components, coil impregnation with an aluminum block, the cryogenic components at 4.2 K, 80 K and 300 K, and the beam duct. The construction and performance of the magnet are detailed below.

1.1 Mechanical design and construction

Figure 2 depicts in three-dimension design and mechanics of SW6. Eight temperature sensors monitor the status of the magnet. These sensors are also to execute the safety protection function. The temperature sensors T1-T4 are PT-100 and T5-T8 Cernox RTDs, in locations shown in Fig. 2. T5 is the upper magnet temperature and T6 and T7 are the temperatures of the two arrays of protection diodes. T8 is bound on the bottom of the LHe transfer tube to monitor the status of the liquid helium filling process. This magnet has an even-number pole design [1], to minimize the field first integral. Poles and coils are impregnated together with an aluminum block [2]. A magnet gap separator made of aluminum bars, maintains a gap of precisely 18 mm between the up and down magnet arrays. Figure 3 shows the cross-section aperture design of the aluminum UHV beam duct and the 4.2 K stainless steel aperture duct. A thermally shielding, especially shaped aluminum beam duct was used to reduce the thermal heating of a cold mass at 4.2 K. Thus, the cold 11 mm vertical aperture of the aluminum beam duct that has 1.2 mm thickness at magnet center region was separated from the cold iron pole and coil by 18 mm.

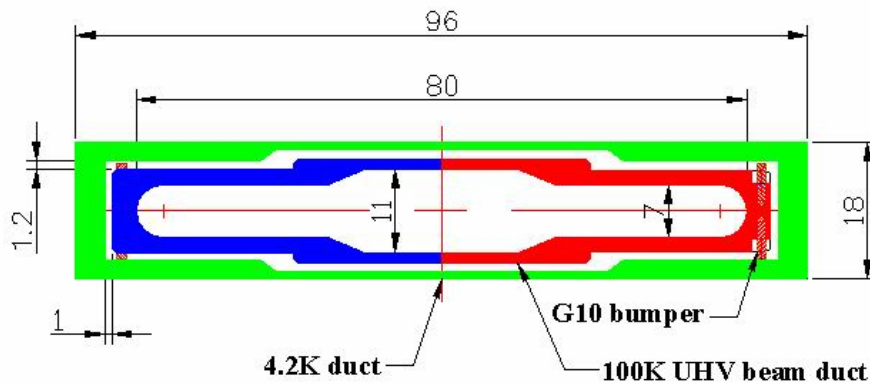


Fig.3. Design cross-section of aluminum UHV beam duct and 4.2 K vessel aperture duct (unit: mm).

A 1.2 mm gap between the Al beam duct and 4.2 K duct prevents the beam duct from touching the 4.2 K aperture duct. Sixteen G10 rod bumpers with a diameter of 1 mm and a length of 5.1 mm were fixed onto the UHV beam duct. The gap between the bumper and the 4.2 K aperture duct was approximately 0.6 mm to ensure that the only point of contact between the beam duct and the 4.2 K duct was the G10 rods that reduce the conducted heat load. The aluminum beam duct was supported and fixed at the both end sides of 4.2 K aperture duct using a G10 with a thickness of exactly 1.2 mm. The Al beam duct was thermally intersected at 100 K by two pieces of copper plates connected to the liquid nitrogen (LN₂) vessel, on both outer ends of the 4.2 K vessel. The flatness in the transverse direction, the pole tilt, the magnet gap, and the variation in the periodic length of magnet in the longitudinal direction of magnet were mechanically measured. Figure 4 plots the errors in the mechanical measurement. The measured data indicate that the rms variation in the periodic length was about 20 μm. The maximum magnetic gap variation in the center region was around 40 μm. The maximum pole tilt was 0.1 mrad. The variation in the electric resistivity of the 64 coils was $8.3 \pm 0.15 \Omega$. These data demonstrate that the constructed magnet meets the specifications.

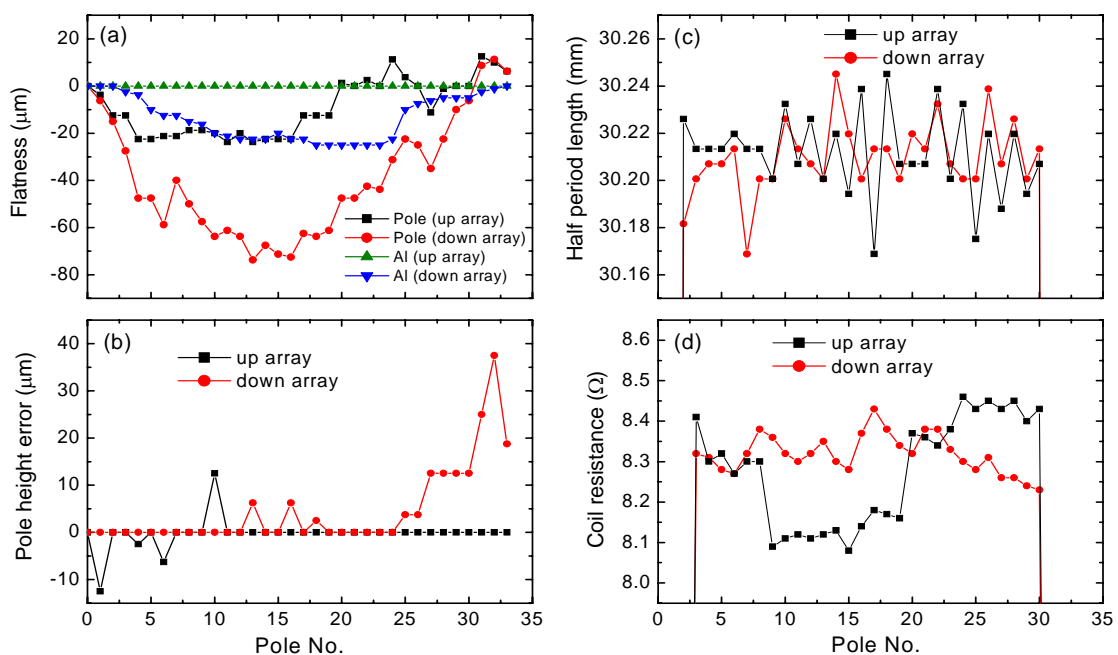


Fig.4. Measured mechanical error on (a) Pole and aluminum block, (b) Pole tilt in x-axis, (c) Periodic length and (d) Coil resistivity measurement on different poles.

1.2 Aluminum beam duct design and construction

The beam duct for the SW6 is made of A6061T5 aluminum alloys (Al), to improve the thermal conductivity and reduce radiation emissivity. A concern has been raised that the pressure inside the cryogenic beam duct would be increased by the re-absorption of the accumulated gas molecules, originally residing on the inner surface of chamber, and their stimulated desorption by scattered synchrotron light when the beam duct is cooled to below 20 K [3]. The dominant residual gases in the NSRRC electron storage ring are H₂ and CO; the number of re-absorbed molecules will be small if the temperature of the beam duct can be kept above 100 K; H₂ and CO are not then frozen on the surface but pumped out. The heat load that crosses the insulation vacuum from the beam duct to the 4.2 K duct vessel is lower for an aluminum beam duct with a lower radiation emissivity, reducing the temperature rise on the 4.2 K vessel duct when the beam duct is irradiated by scattered synchrotron light. Accordingly, the beam duct is designed sufficient space as a vacuum insulation barrier between the beam duct and the 4.2 K vessel duct such that the machining of the beam duct is straighter.

The beam duct is formed by the extrusion method and the outside surfaces are then machined to yield a flatness of < 0.2 mm, to enable it to be inserted inside the 4.2 K aperture duct without touching the 4.2 K duct that is made of SUS304 stainless steel (SS). CNC-machining is applied to the outer surfaces of the Al beam duct in an ethanol sprayed environment to prevent the oil from becoming contaminated. The beam duct is thoroughly chemically cleaned before TIG welding. All the TIG welding of the Al beam duct is performed in the clean room, in which the amount of dust and humidity are carefully controlled. The 4.2 K beam duct transition tapers, made of stainless steel, are joined to the Al beam duct by welding the Al/SS bimetal pieces inside the SW6 and welding the SS-flanges outside the SW6. The temperature of the aluminum beam duct with the stainless steel taper was designed between 300 K and 100 K. The length of the temperature gradient from 80 K to 300 K on both sides of the taper is only 100 mm, which is too short to shield the flow of the heat load from the area at room temperature although a sealed vacuum isolates the tapers from the ambient. Thus the measured temperature of the beam duct is 100 K, which exceeds 80 K. However, no evidence reveals any direct contact between the aluminum beam duct and the 4.2 K vessel duct. Figure 5 presents photographs of (a) the extruded Al beam duct, (b) one side of the Al beam duct joined to the taper by an Al/SS bimetal, (c) on-site TIG welding of the taper and (d) the completed beam duct in SW6.

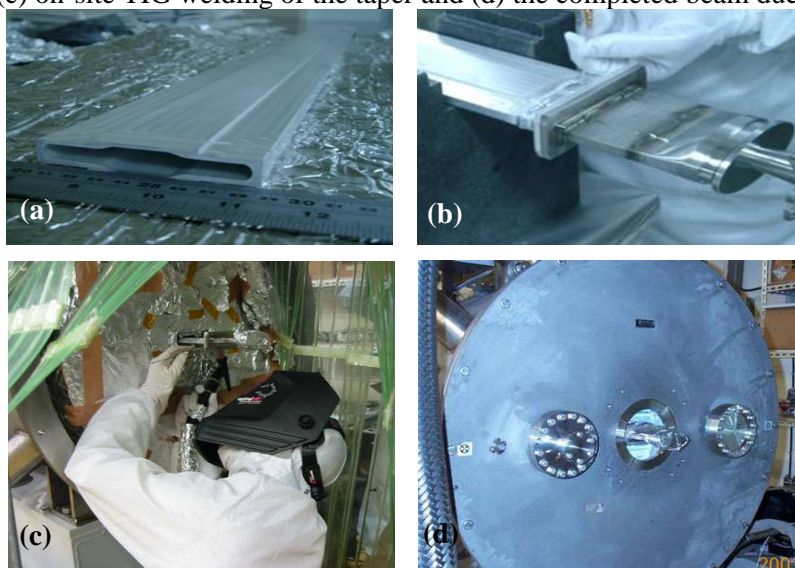


Fig.5. Photographs of (a) extruded Al beam duct; (b) Al beam duct joined to taper by an Al/SS bimetal; (c) on-site TIG welding for the taper; and (d) completed beam duct in SW6.

After the SW6 was installed in the electron storage ring, the UHV beam duct was maintained at room temperature for several weeks to clean the beam duct; cleaning the inner surface of the beam duct reduced the yield of PSD prior to cool down to reduce the number of molecules that could be absorbed on the cryogenic surface during commissioning. The center of the Al beam duct has a temperature of T1 and the two sides of the 80 K thermal intersection have two temperatures of T2 and T3. The up-stream stainless steel taper of the beam duct is at a temperature of T4. The temperature of the whole beam duct is distributed between 300 K and 100 K. When the SW6 was cooled to 4.2 K – the temperature of the Al beam duct was maintained at 100 K. A temperature of the beam duct rose by 1 ~ 1.5 K when the electron beam current was accumulated to 200 mA. The heat load increases the temperature of the beam duct; this increase has two sources – the scattered light and the image current on the beam duct. However, the pressure near the SW6 beam duct does not change, so pressure is not associated with the change of the temperature on the SW6.

1.3 Field measurement

Several field measuring methods including the Hall probe and the stretch wire method were developed to characterize the quality of the field. When the magnet was assembled and enclosed into the vacuum shielding vessel and the liquid helium and nitrogen vessels, a Hall probe [4] was used to measure the field distribution of the magnet at room temperature. A 1 mm-thick flat warm duct with an aperture 57 mm wide and 5.9 mm high was used to isolate the vacuum from the atmosphere. The Hall probe was inserted into the flat warm duct to measure the magnetic field at room temperature [4]. Figure 6 shows the on-axis field measurements and distributions of the second field integrals along the longitudinal axis. The trim coil is not compensated for in determining the field distribution, and the electron beam trajectory simulated based on the measured field is close to the ideal orbit. Hence, the construction performance is quite consistent with the ideal magnet design.

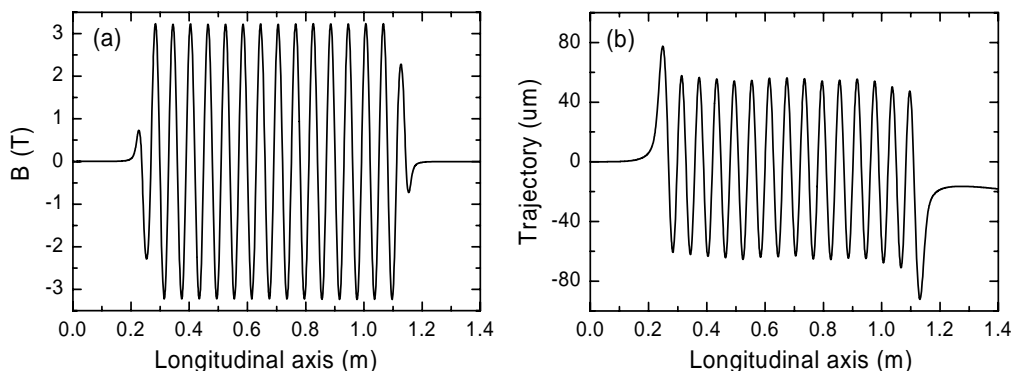


Fig.6. Measured field distribution at room temperature, and calculated electron trajectory along the longitudinal axis, without trim coil compensation.

3. Cryogenic system

A helium cryogenic system that is designed based on the modified Claude cycle provides a maximum cooling power of 450 W at 4.5 K or a maximum liquefaction rate 110 L/h when liquid nitrogen is used in pre-cooling. This helium system keeps the superconducting magnet at 4.3 K (1.085 bar), where the magnet is cooled in the liquefaction mode. The cryogenic system includes one 315 kW compressor, one 45 kW recovery compressor, one 10 kW refrigerator, one 2000 liter dewar, and two 100 m³

helium gaseous buffer tanks. Inside the cold box, two expansion turbines connected in series provide the most of the cooling power for the helium gas stream. The cold box is equipped with two 80 K adsorbers and one 20 K adsorber. The switching and regeneration of the two 80 K adsorbers are fully automatic and can be performed without disturbing the cold box. Two analyzers monitor the impurity of the flowing helium. One analyzer monitors the oxygen and humidity levels at the cold box side; the other monitors the oil aerosol and the nitrogen level at the compressor side. The designed thermal dynamic state and preliminary test results of this helium system can be found in references [5,6].

The system provides a maximum liquefaction rate 139 L/h when liquid nitrogen is used for pre-cooling and a liquefaction rate of 59 L/h without liquid nitrogen. A cooling power of 258 W was obtained at a liquefaction rate of 11 L/h without liquid nitrogen, and a cooling power of 452 W was obtained with a liquefaction rate of 5 L/h using liquid nitrogen. Linearly extrapolating the data yields a cooling power of 327.2 W (469.5 W) in refrigeration mode without (with) liquid nitrogen for pre-cooling. During the measurement of the liquefaction rate and refrigeration capacity without precooling with liquid nitrogen, mass flow rates of 24 g/sec and 44 g/sec, respectively, were observed; values of 39 g/sec and 82 g/sec were obtained with liquid nitrogen pre-cooling. The stand-alone operation of the cryogenic system has the following features. The interlock logic keeps the cryogenic system safe from utility failure and a small-capacity compressor recovers the helium to the storage tanks, maintaining a suction line pressure of 1.1 bar. The emergency power maintains the continuous operation of the control system and the recovery compressor minimizes helium loss in case of an electrical failure. The time required to warm up the cold box to room temperature is 18 hr; naturally warming up the main dewar to room temperature takes 38 days. The initial cooling of the cold box and the main dewar from room temperature to 4.5 K takes 36 hr, and storing the liquid helium to 80 % of the main dewar level with liquid nitrogen precooling takes 10 hr. During the period of liquid helium accumulation, the dewar level sometimes stagnates at 40% and 82%. As the dewar level approaches the maximum set value, the turbines are decelerated and heater is turned on to prevent an over-level event.

A control valve box is connected to the downstream of the multi-channel transfer line. The SW6 and the test dewar are then connected to the valve box via flexible transfer lines. The cold gas from the test dewar is returned to the cold box, while the gas from SW6 returns to the compressor suction line. The operation pressure of the SW6, the test dewar and the main dewar are 1.08 bar, 1.24 bar and 1.4 bar respectively.

4. Magnet testing and commissioning with cryogenic system

A special LHe transfer line is designed to suit operation during both the pre-cooling and the normal auto-filling stages. In the normal filling stage, the two PID controllers are independently associated with LHe and LN₂, used to perform the automatic liquid filling control. This system can also be operated in an on/off-filling mode. LHe filling with PID control is used to keep LHe level at 76% and the on-off control operation mode is used to maintain the LHe level between 65-85%. The magnet has a 200 liters LHe vessel and a 60 liters LN₂ vessel. If the magnet is quenched, the quench signal will be used to close the electro-pneumatic valve of the LHe supply valve and stop the filling of LHe. The commissioning of the SW6 and the cryogenic system is quite successful. Figure 7 shows the training records of the SW6. Magnet quenching vaporized a maximum of 10 liter of liquid helium within 15 seconds. The stored energy of the coil is 50 kJ and part of the stored energy is dumped to the flywheel diode. The diode is cooled partly by liquid helium and partly by cold helium gas. During the training period the cold box and the test dewar were isolated from the SW6 and the compressor was kept running to recover the large amount of the helium gas from the SW6 cryostat. A consumption of more than 60 L/h was required to fill liquid helium to the SW6 cryostat continuously with liquid helium and

maintain a constant level. Most of the helium is vaporized to accommodate the heat loss during the helium transfer phase. A total heat loss of 30 W is estimated for the control valve box, the multi-channel line, the flexible transfer line and the connectors.

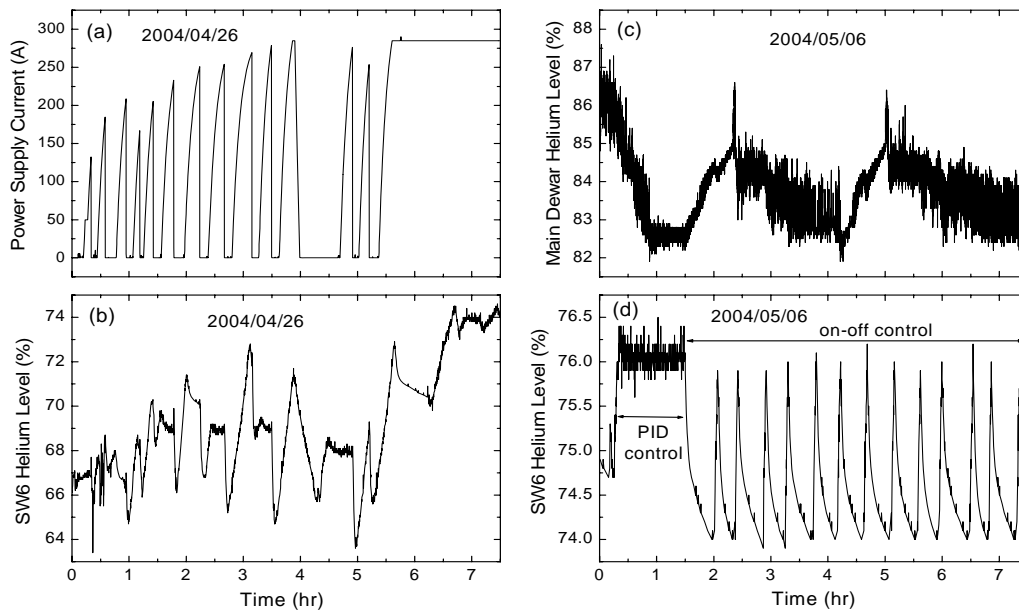


Fig.7. (a) and (b) is the relation between the thirteen quenches and the liquid helium level variation of SW6. (c) and (d) is the relation between the liquid helium filling mode in PID control or on-off control with respect to the liquid helium level variation of the cryogenic system main dewar.

Liquid nitrogen precooling is required to enable the cold box to maintain the main dewar level if no cold gas returns to the cold box. Two strategies are implemented to solve this problem. The by-pass valve is opened in between the helium supply line and the cold return line in the valve box, and the cold gas is allowed to return to the cold box. Meanwhile, the helium level of the SW6 cryostat is regulated in on-off control filling mode with the inlet valve opened at 5% and triggered from a $\pm 1\%$ fluctuation of SW6 cryostat level. SW6 quenching has small effects on the cryogenic system; there are a pressure fluctuation of ± 2 mbar in the suction line, a pressure fluctuation of ± 3 mbar in the main dewar; a temperature increase of 0.3 K in the cold return gas from the valve box, and a fluctuation in the frequency of the cold turbine of ± 10 Hz. The on-off filling mode for SW6 causes a pressure fluctuation of ± 2 mbar at the test dewar.

The operating magnet temperature T5 is about 4.3 K. Moreover, two sensors T6 and T7 on the two protection diodes detect the diode temperature when the magnet quenches. However, the beam duct temperatures with (without) a 200 mA electron beam are about T1=102 K (101 K), T2=100 K (99 K), T3=100 K (99 K) and T4=234.5 K (233 K). The temperature of the beam duct is a function of the electron beam current. The boil-off rates of LHe and LN₂ are around 2.5 L/h and 1.6 L/h as the magnet excitation current is 285 A, respectively. However, the liquid helium consumption from the transfer line is ten times greater than that of the magnet itself. Therefore, the liquid helium transfer system should be modified. The current lead of the magnet is cooled by cold helium gas. Thus, the measured temperature of the return helium gas is around 180 K. The low operation pressure and the high return gas temperature are such that the returned gas from SW6 sent back to the compressor. The cold helium gas is warmed up by a warmer that consisted of a multi-channel aluminum tube, and recycles warm helium gas to the compressor.

The testing of the magnet in the storage ring was quite successful. Thirteen training events yielded a nominal current of 285 A and a field of 3.2 T. No trim coil compensation was involved; the electron beam survived and provided a very stable photon beam for beam line alignment and testing. When the magnet is quenched, the compressor can accommodate a large amount (since 10 liters liquid helium boil-off within 15 seconds) of the recycled helium gas. Regardless of whether beam duct is warm or cold, or whether it has 200 mA electron beams, the UHV pressure of the beam duct is always maintained at a constant value. The commissioning results show that the tune shift effect of SW6 is in good agreement with the model predicted value and there is no unexpected horizontal tune shift caused by the roll-off of the magnetic field. Commissioning with beam was smooth and successful.

5. Conclusions

An aluminum beam duct with temperature of 100 K was designed for use in a superconducting multipole wiggler SW6. No local heating of the aluminum beam duct occurs, preventing an excessive magnet temperature. The pumping and purging of the magnet system include the piping of the transfer line; the return gas should be very carefully maintained at a good dew point and a low particle number to avoid damage to the turbine of the refrigerator. The magnet testing results verify that the magnet construction performance is quite consistent with the ideal design. This result gives us confidence in constructing the superconducting undulator.

6. Acknowledgement

The authors would like to thank the National Science Council of Taiwan for partially supporting this research under Contract No. NSC 92-2112-M-213-019. We would also like to thank Dr. D. J. Wang and Mr. H. C. Ho, C. J for their technical support and Ms. W. P. Li, and P. H. Lin for processing the measured data. We also very appreciate Wang NMR Inc. to construct a high quality magnetic field of the superconducting wiggler for NSRRC.

7. References

- [1]C. S. Hwang, B. Wang, et al., " Design of a superconducting multipole wiggler for synchrotron radiation", IEEE Trans. Appl. Supercond. Vol. 13, No. 2 (2003) 1209.
- [2] C. S. Hwang, B. Wang, et al., "Construction and performance of a superconducting multipole wiggler", AIP, CPC05, Synchrotron Radiation Instrumentation: Eighth International Conference (2004) 199.
- [3]V. Baglin, I.R. Collins, O. Gröbner, C. Grünhagel, B. Jenninger, Vacuum 67 (2002) 421.
- [4]T. C. Fan, F. Y. Lin, M.H. Huang, C.H. Chang, C. S. Hwang, " Magnetic Field Measurement on Superconducting Multipole Wiggler with Narrow Duct ", PAC'2003, Oregon, Portland (2003).
- [5]Hsiao, F. Z., et al., "The Liquid Helium Cryogenic System for the Superconducting Cavity in SRRC", PAC'2001 (2001) 1604.
- [6]Hsiao, F. Z., et al., "The Pilot-Runs of the Helium Cryogenic System for the TLS Superconducting Cavity", PAC'2003, Oregon, Portland (2003).